THE COMPANY OF
Biologists

RESEARCH ARTICLE

GEF-H1 functions in apical constriction and cell intercalations and is essential for vertebrate neural tube closure

Keiji Itoh*, Olga Ossipova* and Sergei Y. Sokol‡

ABSTRACT

Rho family GTPases regulate many morphogenetic processes during vertebrate development including neural tube closure. Here we report a function for GEF-H1/Lfc/ArhGEF2, a RhoA-specific guanine nucleotide exchange factor that functions in neurulation in *Xenopus* embryos. Morpholino-mediated depletion of GEF-H1 resulted in severe neural tube defects, which were rescued by GEF-H1 RNA. Lineage tracing of GEF-H1 morphants at different developmental stages revealed abnormal cell intercalation and apical constriction, suggesting that GEF-H1 regulates these cell behaviors. Molecular marker analysis documented defects in myosin II light chain (MLC) phosphorylation, Rab11 and F-actin accumulation in GEF-H1-depleted cells. In gain-of-function studies, overexpressed GEF-H1 induced Rho-associated kinase-dependent ectopic apical constriction – marked by apical accumulation of phosphorylated MLC, γ-tubulin and F-actin in superficial ectoderm – and stimulated apical protrusive activity of deep ectoderm cells. Taken together, our observations newly identify functions of GEF-H1 in morphogenetic movements that lead to neural tube closure.

KEY WORDS: Neural tube closure, Apical constriction, Epiboly, Cell intercalation, *Xenopus*, Lfc, Myosin II, Rho GTPases, Morphogenesis

INTRODUCTION

Although neural tube defects are among the most common developmental abnormalities, and more than 200 genes have been implicated in this process in mouse genetic models (Harris and Juriloff, 2010), the molecular and cellular events that regulate neural tube closure are poorly understood. The development of the vertebrate central nervous system is a complex process that involves a number of distinct steps. Initially, neural tissue is specified in dorsal ectoderm by secreted factors that are produced by the Spemann organizer (De Robertis and Kuroda, 2004). During gastrulation, neuroectoderm progenitors exhibit complex morphogenetic behaviors to conform to the main embryonic body plan (Gray et al., 2011; Keller et al., 1992a; Poznanski et al., 1997). As development proceeds, apical constriction of neuroepithelial cells, cell intercalations and dorsal convergence drive the appearance of bilateral neural folds and their fusion (Colas and Schoenwolf, 2001; Davidson and Keller, 1999; Keller, 1991; Schroeder, 1970; Suzuki et al., 2012; Wallingford et al.,

Department of Developmental and Regenerative Biology, Icahn School of Medicine at Mount Sinai, New York, NY 10029, USA.
*These authors contributed equally to this work

‡Author for correspondence (sergei.sokol@mssm.edu)

2013). Taken together, these cell behaviors are the main contributors to morphogenetic movements underlying vertebrate neurulation.

One of the crucial regulators of neural tube closure is non-muscle myosin II (Rolo et al., 2009; Tullio et al., 2001). Both intercalatory and constricting cell behaviors require reorganization of many cytoskeletal components and involve dynamic changes in myosin II localization and activity (Lecuit et al., 2011; Rauzi et al., 2010; Vicente-Manzanares et al., 2009). Myosin II controls the contractile force by binding to, and sliding along, actin filaments. Myosin II has also been implicated in a variety of cellular processes – such as cell junction stability, nuclear movement, apical–basal protein targeting – yet there is limited understanding of how myosin II is selectively recruited to perform these specific tasks. Similar to myosin II, small Rho GTPases play essential roles in vertebrate neurulation (Habas et al., 2003; Habas et al., 2001; Hall, 2005; Jaffe and Hall, 2005; Kinoshita et al., 2008). The existence of at least 70 vertebrate guanine nucleotide exchange factors (GEFs) that are related to Dbl (also known as MCF2), which are activators of Rho GTPases, with unique spatiotemporal expression, subcellular localization and diverse specificities presents a significant challenge for studies of the regulation of Rho GTPases in the context of the whole organism (Rossman et al., 2005).

Only a few of the existing RhoA-specific GEFs have been assigned specific developmental functions. The mesoderm-specific WGEF (also known as ARHGEF19) (Tanegashima et al., 2008) and ubiquitous Net1 (Miyakoshi et al., 2004) have been implicated in convergent extension movements. The Rho GEF Trio functions in neural crest migration (Kashef et al., 2009) and apical constriction during optic lens pit invagination (Plageman et al., 2011). In *Drosophila*, RhoGEF2 is essential for the apical constriction that is associated with tissue invagination during gastrulation (Barrett et al., 1997; Häcker and Perrimon, 1998; Kölsch et al., 2007). Although vertebrate neurulation is likely to involve many GEFs, at present, only PDZ-RhoGEF/ArhGEF11 has been implicated in this process in the chicken (Nishimura et al., 2012). In zebrafish embryos, ArhGEF11 morphants do not exhibit defects in neural tube morphogenesis (Panizzi et al., 2007), raising a question as to whether this protein has a conserved role in neural tube closure. In-depth analysis of individual GEF proteins is therefore essential for further understanding of the morphogenetic mechanisms that underlie vertebrate neurulation.

GEF-H1/Lfc/ArhGEF2 is a microtubule-binding Dbl-homology-domain GEF that is specific for RhoA (Birkenfeld et al., 2008; Glaven et al., 1999; Krendel et al., 2002; Ren et al., 1998). In cultured mammalian cells, GEF-H1 has been implicated in cell adhesion (Birukova et al., 2006; Chang et al., 2008) (Yamahashi et al., 2011), cell migration (Heasman et al., 2010; Nalbant et al., 2009; Tsapara et al., 2010), cytokinesis (Birkenfeld

Journal of Cell Science

et al., 2007), junctional communication (Aijaz et al., 2005; Benais-Pont et al., 2003; Guillemot et al., 2008) and vesicular trafficking (Pathak et al., 2012). Despite these crucial roles of GEF-H1 in regulating cell shape and behavior *in vitro*, its involvement in morphogenetic processes *in vivo* has not been investigated. Because GEF-H1 RNA is expressed in the early ectoderm, and the neural plate, of *Xenopus* embryos (Morgan et al., 1999), we investigated a possible role for GEF-H1 in neurulation. In this study, we demonstrate that depletion of GEF-H1 from *Xenopus* embryos interferes with morphogenetic cell movements, including cell intercalation and apical constriction, thereby leading to neurulation defects. In gain-of-function studies, overexpression

of GEF-H1 efficiently induces Rho-associated kinase (ROCK)–myosin-II-dependent apical constriction in embryonic ectoderm and stimulates the protrusive activity of deep ectoderm cells. These observations reveal an important role for GEF-H1 in morphogenetic events that accompany vertebrate neural tube closure.

RESULTS

Depletion of *Xenopus* GEF-H1 results in neural tube closure defects

GEF-H1 RNA is expressed in the neural tissue of *Xenopus* embryos (Morgan et al., 1999), indicating a possible function
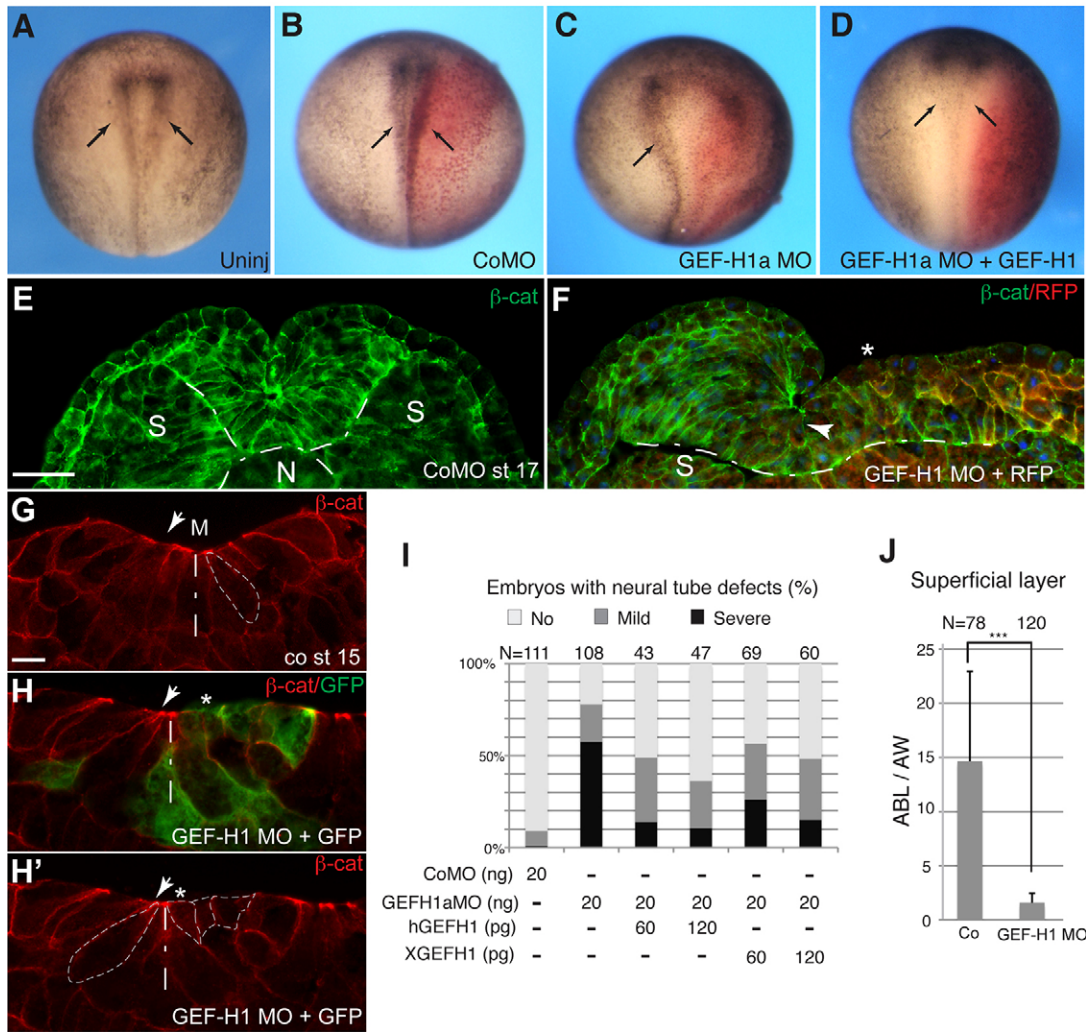
Fig. 1. Neural tube defects in embryos depleted of GEF-H1. (A) Uninjected embryo at stage 16. (B–D) Four-cell embryos were unilaterally injected with control (CoMO) (B), or GEF-H1a (GEF-H1a MO) (C,D) morpholino oligonucleotides (20 ng each) and *LacZ* RNA (40 pg). (D) Human GEF-H1 RNA (60 pg) rescued the neural fold defect that was caused by GEF-H1a MO. The dorsal view is shown, anterior is to the top. Arrows point to the neural folds. (E,F) Neural fold morphology in stage-17 (st 17) embryos that had been injected with CoMO (40 ng) (E) or GEF-H1 MO (F) (40 ng) was visualized by using β-catenin staining (green). Membrane-associated RFP RNA (160 pg) (F) marks the injected side of the embryo. N, notochord; S, somite. Tissue boundaries are demarcated by broken lines. Arrowhead points to constricting cells, * lack of apical constriction. (G,H) Constricted cell morphology in the cross-sections of neurula embryos (stage 15) that had been unilaterally injected with GEF-H1 MO (40 ng). (G) control (co) embryo. (H) GFP (green) is a lineage tracer, (H′) red channel only of H. The broken lines in G and H′ show the cell boundaries. M, midline position, dorsal is at the top. Arrows point to constricting cells, * lack of apical constriction. (I) Quantification of neural fold defects caused by the injection of GEF-H1a MO and the rescue with human or *Xenopus* GEF-H1 RNA. Morpholino oligonucleotides and RNAs were injected at the indicated doses. Neural tube defects were scored at stages 16–18 as described in supplementary material Fig. S1. The number of embryos that were scored is shown along the top. (J) Quantification of cell shape in superficial neuroectoderm from GEF-H1-MO-injected or control uninjected sides. Results are expressed as the ratios of apical-basal length over the apical width (ABL/AW) in four to six superficial cells that were located adjacent to the midline. Means±s.d. are shown. Cells were scored in 8–11 sections from three embryos, with the total cell number shown on top of each group. Statistical significance was assessed by using Student's *t*-test, *P*<0.0001. Scale bars: 100 μm (E); 20 μm (G).

during neural tube formation. To study the developmental roles of GEF-H1, we depleted the *Xenopus* GEF-H1 protein with antisense morpholino oligonucleotides. Because there are two *Xenopus laevis* GEF-H1 cDNAs (a and b, see Materials and Methods), which differ in their 5'-untranslated sequence and several N-terminal amino acids, we used morpholino oligonucleotides that targeted different sequences. Using the morpholino oligonucleotides GEFH1 MO and GEF-H1a MO, which both targeted the GEF-H1a isoform, we observed dose-dependent neural fold defects in embryos that had been unilaterally injected with both morpholino oligonucleotides compared with the control siblings (Fig. 1A–C,F; supplementary material Fig. S1A and Movie 1). Similar neural tube defects were seen upon using the morpholino oligonucleotide GEF-H1b MO, which targets a different protein isoform and synergized with the GEF-H1a MO in co-injection experiments (supplementary material Fig. S1A). GEF-H1a MO and GEF-H1 MO efficiently inhibited *Xenopus* GEF-H1a RNA translation *in vivo* (supplementary material Fig. S1B), and both were used in subsequent loss-of-function studies. Importantly, co-injection of human GEF-H1 or *Xenopus* GEF-H1 RNAs lacking the morpholino target sequence significantly rescued neural tube defects in GEF-H1-MO-injected embryos (Fig. 1D,I).

We examined cell and tissue morphology in stage-17 neurulae that had been unilaterally injected at the 4–8-cell stage with GEF-H1 MO and membrane-associated red or green fluorescent protein (RFP and GFP, respectively) RNAs as lineage tracers. Cryosections demonstrated that the neural fold failed to close at the GEF-H1-MO- or GEF-H1a-MO-injected side compared with the uninjected side or control-MO-injected embryos

(Fig. 1F–H; supplementary material Fig. S1A,C). Examination of the superficial cell morphology confirmed a defect in apical constriction, an important cell behavior that accompanies neural tube closure (Fig. 1G,H,J).

To confirm neural tube closure defects in GEF-H1-MO-injected embryos using a different assay, we visualized the neural plate boundary by whole-mount *in situ* hybridization for *Sox2* (a pan-neural-tissue marker; Fig. 2). *Sox2* was more broadly distributed and less intensely stained at the side of the embryo that had been injected with either of the two GEF-H1 morpholino oligonucleotides compared with the control side (Fig. 2A,D,E), which is consistent with the observed neural folding defects. All three morpholino oligonucleotides produced similar defects on the width of the *Sox2* expression domain (Fig. 2A,D,E; data not shown). This defect was rescued by wild-type human GEF-H1 but not by the inactive form of human GEF-H1, which has the mutation Y393A (Fig. 2A–C,F), further suggesting that GEF-H1 activity is required for the morphogenetic behaviors that accompany neural fold formation. Taken together, these results reveal an essential role of GEF-H1 in cell shape changes that are associated with neural tube closure.

GEF-H1 regulates neural tube closure by affecting different cell behaviors

In order to understand how GEF-H1 depletion leads to neural tube closure defects, we wanted to examine specific cell behaviors in GEF-H1-depleted tissues at different developmental stages. Besides the altered cell shape in the closing neural tube in GEF-H1 morphants, we studied the effect of GEF-H1 morpholino oligonucleotides on apical constriction using several markers of
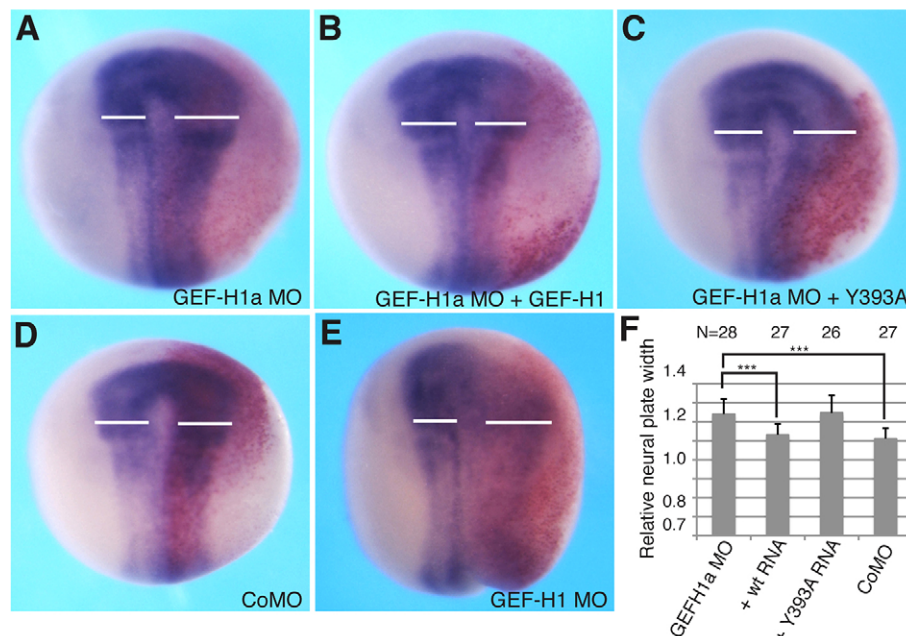
Fig. 2. Changes in the *Sox2*-positive domain in GEF-H1 morphants. (A–E) Embryos were injected laterally into two sites at the four-cell stage with *LacZ* RNA as lineage tracer (40 pg) and morpholino oligonucleotides or RNAs as indicated. Doses were as follows: (A–C) GEF-H1a MO and (D) CoMO (control) (20 ng), (E) GEF-H1 MO (40 ng) and human GEF-H1 RNA (GEF-H1; wt) (60 pg) or human GEF-H1-Y393A RNA (Y393A) (800 pg). Whole-mount *in situ* hybridization with a *Sox2* probe at stages 14–15 is shown, β-galactosidase activity (red) marks the injected side. A dorsal view is shown, the anterior is top. (B) Wild-type human GEF-H1 but not the (C) inactive GEF-H1-Y393A RNA reverses the morphant phenotype (A). (A–E) White bars indicate the width of the *Sox2* expression domain at the level of the mid-hindbrain boundary. (F) Quantification of embryo phenotypes. The *Sox2* domain was measured at the mid-hindbrain boundary as indicated in A–D. The ratios of the *Sox2* domain width on the injected side over that on the uninjected side are shown. A ratio of 1.0 indicates equal width of the *Sox2* domain on both sides. Statistical significance was assessed by using Student's *t*-test. ***$P < 0.0001$. The *n* values are shown across the top of the graph and indicate the number of embryos that were measured.

apical constriction (Fig. 3). We observed that the superficial neural plate cells on the side that had been injected with GEF-H1 MO failed to express phosphorylated regulatory myosin II light chain (MLC) and F-actin, known molecular markers of apical constriction (Choi and Sokol, 2009; Lee and Harland, 2007) (Fig. 3A–D). Additionally, the superficial cells did not accumulate Rab11, a recycling endosome marker that has been implicated in neural tube closure (Ossipova et al., 2014) (Fig. 3E,F). By contrast, these markers and tissue morphology were not affected by injection of the control MO (supplementary material Fig. S1D–F). Taken together with the previously shown cell morphology data (Fig. 1G,H,J), these findings further support the conclusion that the apical constriction of neural plate cells is abnormal in GEF-H1 morphants.

In addition to neural tube closure defects, we observed that non-neural ectoderm contains three to seven cell-layers at the GEF-H1-MO-injected side, in comparison with two cell-layers in the uninjected tissue in the majority of the injected embryos ($n{>}30$) (Fig. 4A–C; supplementary material Fig. S2A,B). Of note, the lateral plate mesoderm was also wider at the injected side. The same effects were seen with GEF-H1a MO, but not with the control MO (data not shown). These observations suggest that, in addition to apical constriction, GEF-H1 is involved in cell intercalations, which occur both in neural and non-neural tissues. To exclude the possibility that GEF-H1 has an inhibitory effect on cell divisions, we assessed the number of mitotic cells by staining embryo sections with an antibody against phosphorylated histone 3 (H3), which recognizes only mitotic nuclei (Saka and Smith, 2001). The number of phosphorylated-H3-positive cells was not significantly different at the side that had been injected with the morpholino oligonucleotide versus that of the uninjected side (supplementary material Fig. S2C,D). These results suggest

that GEF-H1 regulates cell behaviors in both neural and non-neural tissues.

Epiboly is an early morphogenetic process that is driven by radial cell intercalations, which convert multilayered blastula ectoderm into two cell-layers that eventually spread over the entire embryo surface during gastrulation (Keller, 1991). To assess the involvement of GEF-H1 in epiboly, we studied clone spreading in stage-11 embryos that had been unilaterally injected with GEF-H1 morpholino oligonucleotides at the four- to eight-cell stage and then injected bilaterally with *LacZ* RNA at the 16-cell stage (Fig. 4D). The side that received either of the two GEF-H1 morpholino oligonucleotides consistently showed more restricted distribution of β-galactosidase-positive cells in 30 out of the 35 examined embryos by contrast with that of the control side. This was confirmed by measuring the β-galactosidase-positive area at the uninjected side and at the side where GEF-H1 morpholino oligonucleotides had been injected (Fig. 4E,F; data not shown). These results suggest that GEF-H1 is required for early cell intercalations, which normally lead to dispersion of the clones before the midgastrula stage. Embryo cryosections revealed four to six ectodermal cell-layers in gastrula tissues that had been depleted of GEF-H1; by contrast, uninjected tissues had only two to three cell-layers (Fig. 4A–C; supplementary material Fig. S2A,B). These changes were visible as early as stage 10 in all sectioned embryos ($n{=}35$), indicating that GEF-H1 is required in order for ectoderm to undergo radial intercalations. This epiboly defect might, therefore, contribute to subsequent neural tube closure.

We next investigated whether GEF-H1 is involved in other types of cell intercalatory movements, such as mesodermal convergent extension (Keller, 2002). To investigate whether this cell behavior requires GEF-H1, we studied *Xenopus* ectodermal
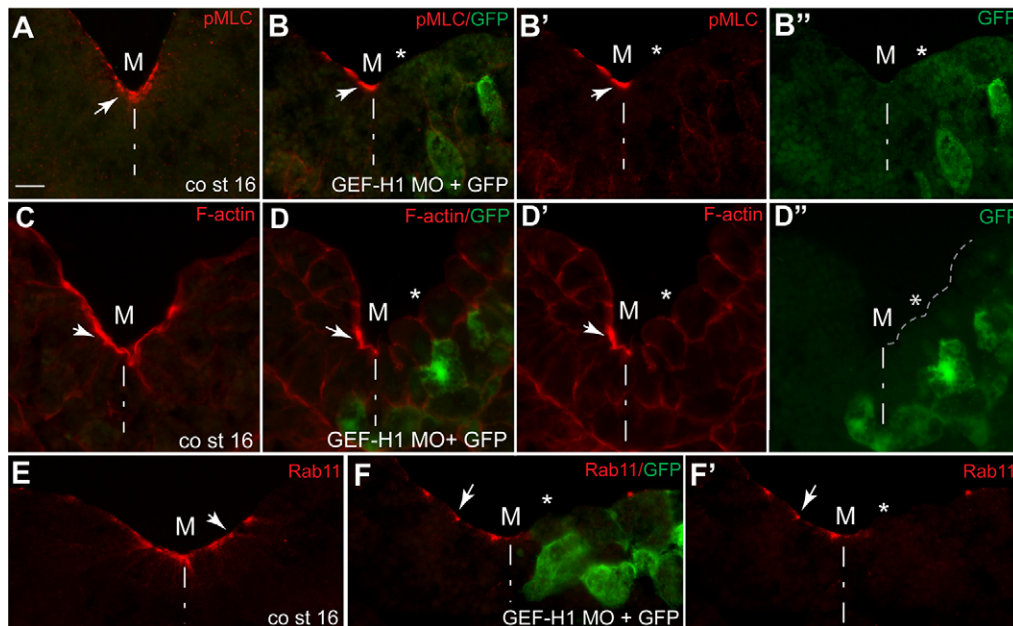
Fig. 3. Depletion of GEF-H1 interferes with apical constriction in the neural plate. Four-cell embryos were unilaterally co-injected with 40 ng of morpholino oligonucleotide against GEF-H1 (GEF-H1 MO) and 200 pg of GFP RNA (as a lineage tracer; green). Immunostaining of transverse neural fold sections (in stage-16 embryos) for apical constriction markers. The uninjected side served as a control (co st 16). Arrows point to the uninjected area, * cells that had been injected with GEF-H1 MO. The midline (M) is indicated by the broken line. (A,B) phosphorylated myosin II light chain (pMLC; red), (C,D) F-actin, (E,F) Rab11. Control-MO-injected embryos (supplementary material Fig. S1D–F) were indistinguishable from the uninjected embryos. B′, D′, F′ show the images in the corresponding panel in the red channel only; B″ and D″ show the images in the corresponding panel in the green channel only. Scale bar: 20 μm.
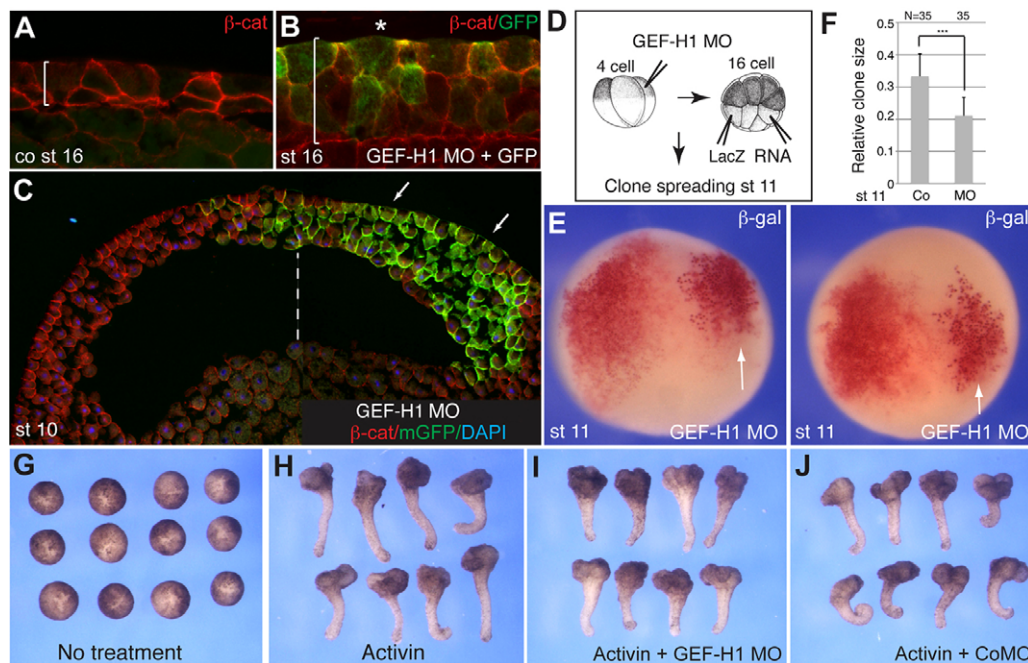
Fig. 4. GEF-H1 functions to regulate radial cell intercalations. (A) Embryonic ectoderm at stage 16 (st 16) that had been injected with the control morpholino oligonucleotide (co). (B) GEF-H1-depleted embryo (GEF-H1 MO) contains abnormally thick ectoderm at stage 16. GFP was injected as described in the Fig. 3 legend. (C) The role of GEF-H1 in epiboly. Eight-cell embryos ($n>20$) were injected with 20 ng of GEF-H1 MO with 150 pg of membrane associated GFP RNA (mGFP; green) as a tracer into one dorsal animal-pole blastomere. Cross-section of a representative injected embryo (stage 10) stained for β-catenin (red) to mark cell boundaries. Up to eight cell layers are visible at the site of GEF-H1 MO injection (arrows) as compared with the uninjected side, which contains 3–4 layers. The animal pole is at the top. Dashed line indicates midline. DAPI staining is blue. (D) Scheme of experiments shown in E and F. Four-cell embryos were injected unilaterally in animal-dorsal blastomere with the GEF-H1 MO (40 ng), followed by bilateral injection of *LacZ* RNA (25 pg) at the 16-cell stage. At stage 11, clone distribution was revealed by staining for β-galactosidase (β-gal) activity. (E) Clone dispersion is defective at the GEF-H1-depleted side of the embryo at stage 11 (arrows). Two representative embryos are shown. The animal pole is to the top, dorsal view. (F) Quantification of the experiment shown in D and E. The results are shown as the mean diameters of the β-galactosidase-positive areas±s.d. relative to the whole embryo size, the number of embryos that was investigated is shown across the top. Statistical significance was assessed by using Student's *t*-test, ***$P<0.001$. (G–J) GEF-H1 is not required for animal cap elongation in response to activin A. Four- to eight-cell embryos were injected into four animal-pole sites with 20 ng of GEF-H1 MO or the control morpholino oligonucleotide (CoMo) as indicated. Animal cap explants were prepared at stage 8 and treated with activin A (0.5 ng/ml). Explant morphology was visualized when uninjected embryos reached stage 16.

explant elongation in response to activin A (a mesoderm inducing factor), which is a useful test for morphogenetic cell behavior (Howard and Smith, 1993; Sokol, 1996). Surprisingly, we observed no significant effect of GEF-H1 MO on activin-A-induced explant elongation (Fig. 4G–J). By contrast, Xdd1 (a truncated form of *Xenopus* Dvl2) efficiently inhibited this behavior (Sokol, 1996; data not shown). These observations support a selective role of GEF-H1 in radial intercalations and apical constriction, but not in activin-dependent convergent extension of mesodermal cells.

GEF-H1 triggers ectopic apical constriction in embryonic ectoderm

To initiate the analysis of the pathway used by GEF-H1, we wanted to establish a gain-of-function assay for GEF-H1 activity *in vivo*. To prevent GEF-H1 inhibition by associated microtubules, we used constitutively active human GEF-H1 with the C53R mutation (GEF-H1-C53R) (Krendel et al., 2002). RNAs encoding GEF-H1-C53R or wild-type *Xenopus* GEF-H1 were microinjected into animal blastomeres of four-cell embryos. By the onset of gastrulation, both RNAs caused tissue bending at the site of injection, accompanied by increased pigment granule accumulation (Fig. 5A,B). These morphological changes are characteristic of apical constriction (Lee and Harland, 2007; Sawyer et al., 2010). Indeed, these effects of GEF-H1 were

indistinguishable from the activity of Shroom, an actin-binding PDZ domain-containing protein that is known to trigger apical constriction (Haigo et al., 2003; Hildebrand and Soriano, 1999) (Fig. 5C). The effects of *Xenopus* wild-type GEF-H1 and constitutively active forms of human and *Xenopus* GEF-H1 were similar (data not shown), suggesting that wild-type GEF-H1 is not inhibited by microtubules in our experimental setting. The inactive forms of human and *Xenopus* GEF-H1, which have mutations in the Dbl homology domain that abolish nucleotide exchange activity of GEF-H1 (Krendel et al., 2002), did not alter the normal appearance of the injected ectoderm, demonstrating that the effect requires the Rho GEF activity of GEF-H1 (supplementary material Fig. S3A–C; data not shown). Examination of transverse cryosections confirmed that the superficial cell layer that expressed GEF-H1 frequently contained cells that were elongated along the apico-basal axis and comprised a reduced apical surface ('bottle cell' morphology) by comparison to that of the uninjected controls or cells that had been injected with the inactive form of human GEF-H1 (Y393A) (Fig. 5D–J; data not shown). These observations suggest that GEF-H1 is sufficient to stimulate ectopic apical constriction in *Xenopus* embryonic ectoderm.

To investigate how GEF-H1 triggers apical constriction, we first determined its subcellular localization in ectodermal cells. As the endogenous protein was not detected by using commercial
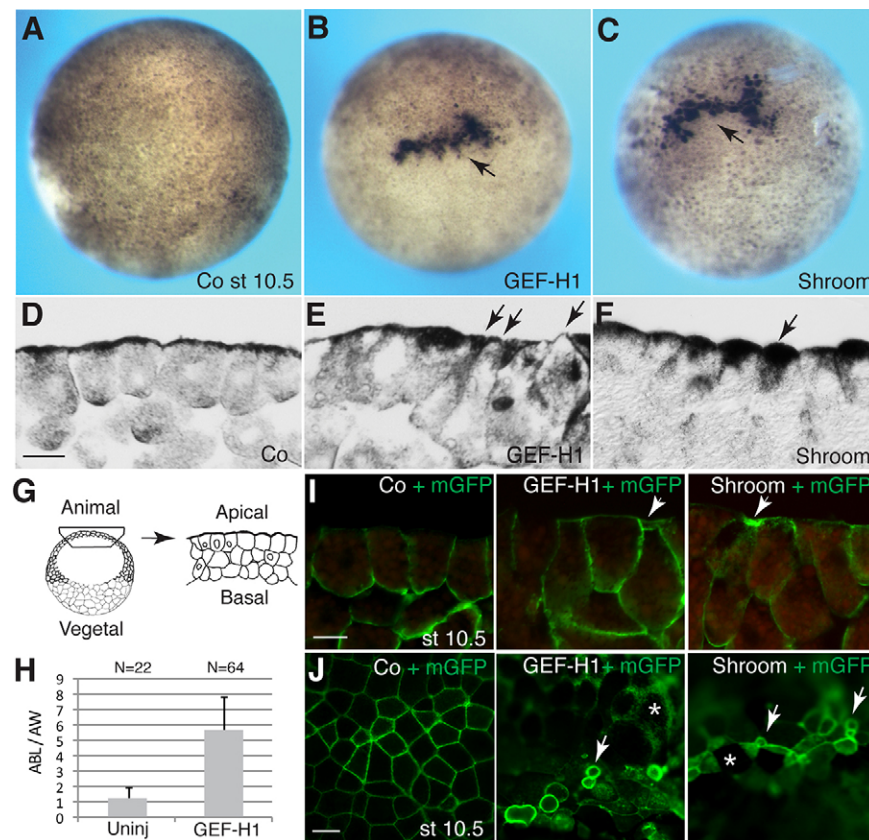
Fig. 5. GEF-H1 induces ectopic apical constriction in ectodermal cells. (A–C) Ectopic apical constriction induced by GEF-H1 and Shroom in ectoderm. Four-cell embryos were injected with RNAs and cultured until late-blastula or early-gastrula stages (9–10+). (A) Uninjected control (Co) embryo. (B) Embryo injected with *Xenopus* Myc–GEF-H1 RNA (50 pg). (C) Embryo injected with Shroom RNA (200 pg). Arrows point to the areas undergoing apical constriction. Top view is shown. (D–G) Cross-sections of embryos that had been injected with human GEF-H1-Y393A (D) or human GEF-H1-C53R (E) or Shroom (F) RNA. Ectoderm cells accumulate pigment at the apical surface and reduce their apical surfaces (arrows). Human GEF-H1-Y393A-expressing cells are indistinguishable from control uninjected ectoderm. (G) Scheme of the experiments showing the tissue sectioned in (D–J), apical is up. (H) Quantification of cell shape in GEF-H1-expressing and control (uninj) cells. Results are expressed as ratios of apical-basal cell length over apical width (ABL/AW) in the superficial layer cells (as shown in D and E). Means±s.d. are shown. The numbers above the bars indicate the number of cells counted per group (*n*). Five GEF-H1-expressing and two control embryos were examined. Statistical significance was assessed by Student's *t*-test, $P<0.0001$. (I) Morphology of cells that underwent apical constriction (arrows) from embryos that had been injected with *Xenopus* Myc–GEF-H1 (50 pg) or Shroom (200 pg) RNAs as indicated. The cell membrane is marked by co-expression of membrane-targeted GFP (mGFP), which was detected by using an antibody against GFP (green). Co, control ectoderm. (J) *En face* views of ectoderm from the experiment in I. Arrows point to cells that express *Xenopus* Myc-GEF-H1 or Shroom with membrane-associated GFP (mGFP). Live embryos are shown. * uninjected cells. Scale bars: 20 μm.

antibodies, we visualized epitope-tagged GEF-H1 after it had been expressed in embryonic ectoderm. Both Myc- and hemagglutinin (HA)-tagged GEF-H1 proteins were enriched near the apical surface of the constricting superficial cells, in addition to the cytoplasmic and cortical localization in both superficial and inner ectoderm (Fig. 6A,B; data not shown). Inactive *Xenopus* Myc–GEF-H1 with the mutation Y444A was mostly cytoplasmic with little cortical localization (supplementary material Fig. S3D,E). These observations suggest that apically localized GEF-H1 promotes the formation of the apical actomyosin contractile network that is essential for apical constriction. We therefore stained for the presence of F-actin and phosphorylated MLC at the apical surface. Both markers were detectable in hyper-pigmented cells that expressed low amounts of GEF-H1, yet they were absent from the apical surface of the uninjected tissue (Fig. 6C,D,F,G). Consistent with these findings, the overexpression of GEF-H1 and ROCK also increased the levels of phosphorylated MLC in western blot assays (Fig. 6E). Additionally, the injection of GEF-H1 RNA

resulted in the accumulation of γ-tubulin, which has been implicated in the formation of polarized microtubule arrays in cells that constrict in response to Shroom (Lee et al., 2007a) (Fig. 6H,I). These results support the possibility that GEF-H1 acts to locally activate actomyosin contractile filaments, which mediate apical constriction.

ROCK is involved in GEF-H1-dependent apical constriction
ROCK is a key effector of RhoA, which promotes the phosphorylation of the regulatory MLC (Vicente-Manzanares et al., 2009). We therefore tested the involvement of ROCK in GEF-H1-induced apical constriction. An N-terminal truncation form of ROCK, which acts in a dominant-negative manner (Marlow et al., 2002), efficiently inhibited the apical constriction induced by either human or *Xenopus* GEF-H1 RNAs (Fig. 7A–D; data not shown). Alone, dominant-negative ROCK caused depigmentation of blastula ectodermal cells (Fig. 7C). The levels of phosphorylated MLC were increased in ectodermal cells that expressed active GEF-H1, but not in those that
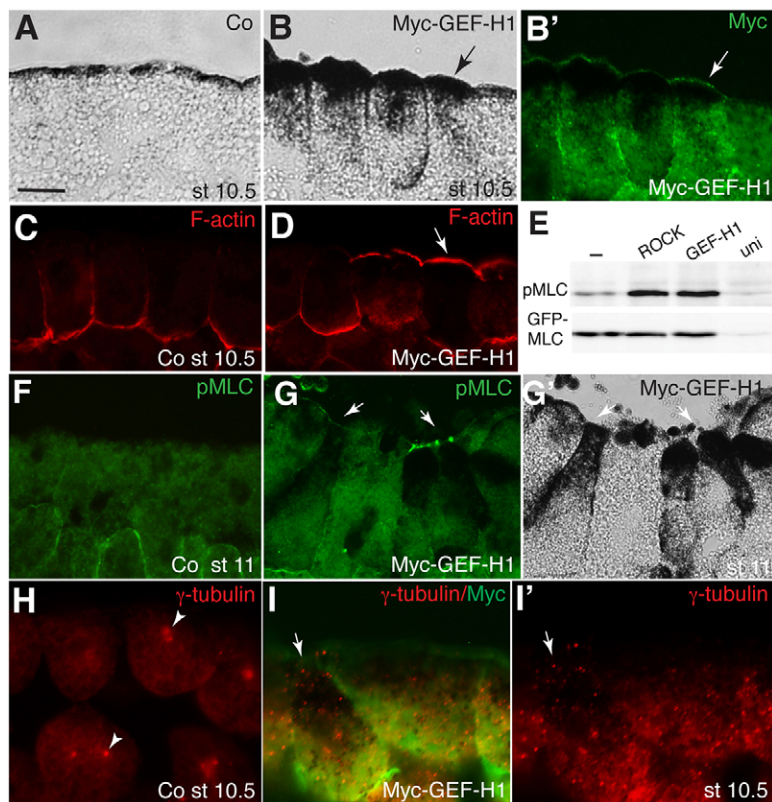
Fig. 6. GEF-H1 activates actomyosin contractility in superficial ectoderm. (A,B) Cross-sections of superficial ectoderm that expressed *Xenopus* Myc-GEF-H1 RNA (25–50 pg). RNA injections were as described in the Fig. 5 legend. (A) Brightfield image of uninjected ectoderm (Co). (B) Brightfield view of GEF-H1-expressing cells that are elongated and highly pigmented. (B′) Myc-staining shows apical enrichment of *Xenopus* Myc-GEF-H1 in constricting cells, which are elongated and heavily pigmented (arrow). (C,D) Accumulation of apical F-actin (red) revealed by Phalloidin staining (arrow) in cross-sections of *Xenopus* Myc-GEF-H1-expressing ectoderm (D), but not in uninjected control tissue (C). (E) GEF-H1 and ROCK activate MLC phosphorylation (pMLC). Immunoblot analysis of lysates of stage-11 embryos, which had been injected with GEF-H1 and ROCK RNA, using antibodies against phosphorylated MLC. No change in total GFP–MLC levels is detected (antibody against GFP). (F,G) Accumulation of pMLC (green) in GEF-H1-expressing cells. (F) Control uninjected embryonic ectoderm. (G) Accumulation of pMLC at constricted apical surfaces (arrows) of *Xenopus* Myc-GEF-H1-expressing cells. G′, Brightfield reveals elongated 'bottle cell' morphology (arrows) with reduced apical surfaces and increased pigmentation. (H,I) GEF-H1 induces γ-tubulin redistribution (red). (H) Control ectoderm at stage 10.5 showing centrosomal localization (arrowheads). (I,I′) Myc-GEF-H1 RNA-injected ectoderm with constricting cells (arrow). I′ shows the red channel only. Scale bars: 20 µm.

expressed the inactive mutant (Fig. 6E–G and Fig. 7E). This ability of GEF-H1 to stimulate phosphorylation of MLC was also blocked by dominant-negative ROCK. Finally, we carried out transcriptional assays in *Xenopus* ectoderm cells that transiently expressed the serum response factor (SRF) and luciferase (SRF-Luc) reporter (Krendel et al., 2002; Posern et al., 2002; Posern and Treisman, 2006). GEF-H1 efficiently upregulated SRF-Luc but not the control reporter, which had mutated SRF-binding sites. This reporter activation required ROCK (Fig. 7F). Taken together, these results strongly indicate that GEF-H1 induces ectopic apical constriction through the activation of the RhoA–ROCK–myosin-II signaling pathway.

GEF-H1 controls intercalatory behavior by modulating myosin II activity in deep ectodermal cells

To further investigate how GEF-H1 regulates cell intercalations, we assessed the staining of phosphorylated MLC in deep ectoderm cells, in which we have manipulated GEF-H1 activity in gain- and loss-of-function experiments. At stages 10–11, deep ectoderm cells exhibited polarized MLC phosphorylation, with a lack of staining in the basal domain (Fig. 8A; supplementary material Fig. S4). Given the key role of phosphorylated MLC and myosin II in cell intercalations, this polarity might reflect the ability of these cells to intercalate between cells that are located more apically. We observed that overexpressed GEF-H1 marked apical cell protrusions that did not contain phosphorylated MLC (Fig. 8B). Such protrusions were much more frequent in cells that expressed GEF-H1 by comparison with those that had not been injected (more than 30 embryos examined), indicating that GEF-H1 stimulates the protrusive activity in deep ectodermal cells. Moreover, in GEF-H1-MO-injected cells, but not in control-MO-injected cells, phosphorylated MLC staining was disorganized (Fig. 8C,D). These observations indicate that, similar to apical

constriction defects, the abnormal radial intercalation of GEF-H1 morphants that is revealed at early-gastrula stages is probably due to the inhibition of MLC phosphorylation.

DISCUSSION

This study addressed the functions of GEF-H1, a RhoA-specific GEF, in *Xenopus* embryogenesis. The knockdown of GEF-H1 resulted in neural tube defects, which are probably caused by abnormal cell intercalations and defective apical constriction in GEF-H1-depleted neuroectoderm. In gain-of-function experiments, we showed that GEF-H1 stimulates ectopic apical constriction in *Xenopus* ectoderm. Taken together, our experiments demonstrate a crucial role for GEF-H1 in cell behaviors that lead to vertebrate neural tube closure. These observations differ from those that have been previously reported for GEF-H1. One study has reported a modest effect of murine GEF-H1/Lfc on ectodermal competence in response to neural inducers (Morgan et al., 1999). Two other studies have proposed a role for GEF-H1/Lfc in inhibiting convergent extension movements in response to microtubule depolymerization; however, the depletion of the reported GEF-H1 variant did not perturb normal embryonic development (Kwan and Kirschner, 2005; Zhou et al., 2010). Because the previously described GEF-H1 cDNA sequence is not present in the National Center for Biotechnology Information (NCBI) databases, it is likely to encode a rare isoform of the protein.

Apical constriction is a morphogenetic process that underlies epithelial tissue folding in diverse developmental contexts, including neural tube closure (Lee and Harland, 2007; Sawyer et al., 2010). GEF-H1-initiated apical constriction is ROCK-dependent and leads to myosin II activation. So far, only a handful of proteins have been shown to trigger ectopic apical constriction. One of these proteins is Shroom (Haigo et al., 2003; Hildebrand, 2005; Hildebrand and Soriano, 1999), which has
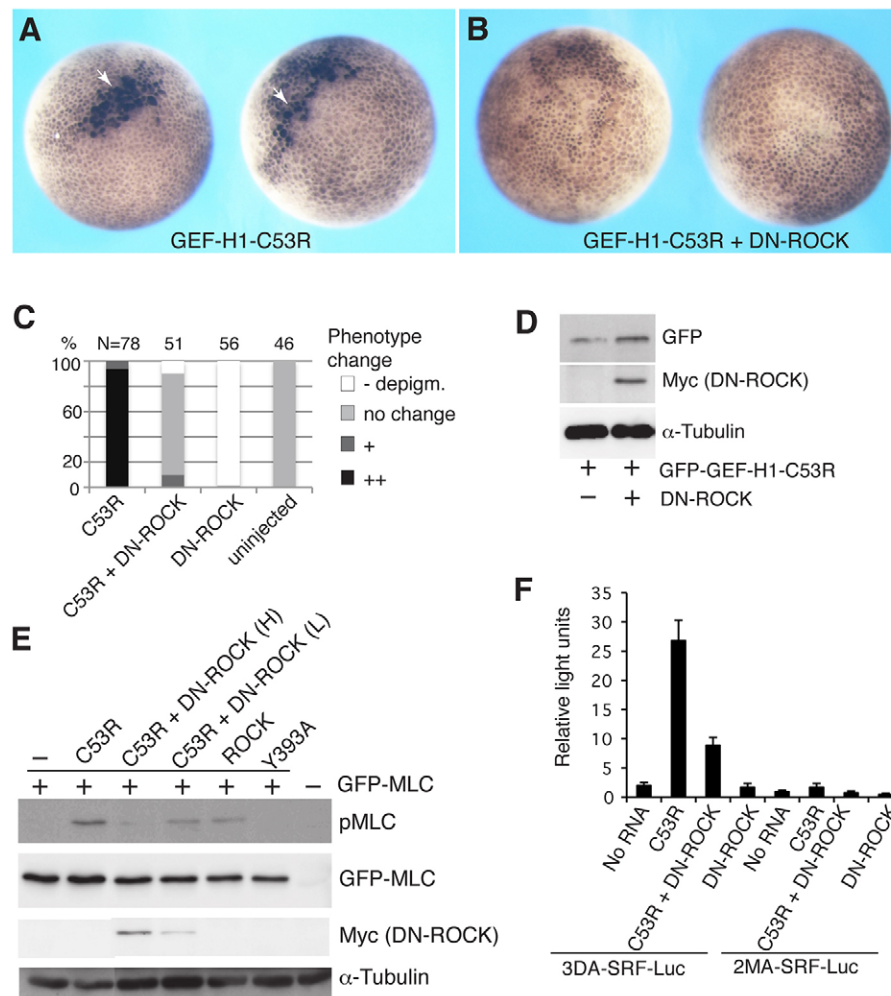
Fig. 7. ROCK is required for GEF-H1-induced ectopic apical constriction. (A,B) Four-cell embryos were injected with GEF-H1-C53R (60 pg) and/or dominant-negative ROCK (DN-ROCK, 400 pg) RNAs into two animal-ventral blastomeres. The animal pole view of stage-8.5 embryos is shown. (A) Intense pigmentation (arrows) accompanies apical constriction in response to expression of GEF-H1-C53R. (B) Dominant-negative ROCK completely blocks the effect of active GEF-H1. (C) Quantification of phenotypic changes for embryos that had been injected with the indicated RNAs. Scoring: ++, hyper-pigmentation; +, weak hyperpigmentation; no change, normal morphology; −, de-pigmentation. Pigment accumulation was associated with apical surface reduction and constriction. The y-axis shows the percentage of embryos with the indicated phenotype. The numbers across the top indicate the total number of embryos examined. (D) Protein levels for GFP-GEF-H1-C53R and Myc-tagged dominant-negative ROCK were assessed by using antibodies against GFP and Myc in embryo lysates taken from experiments performed in A and B. (E) Dominant-negative ROCK suppresses GEF-H1-dependent MLC phosphorylation (pMLC). Four-cell embryos were injected into four animal blastomeres with RNAs encoding GFP–MLC (250 pg), GEF-H1-C53R (C53R, 60 pg), GEF-H1-Y393A (Y393A, 500 pg), dominant-negative ROCK (400 pg, H, high dose; 200 pg, L, low dose), or wild-type ROCK (ROCK, 250 pg) as indicated. Injected embryos were lysed at stage 8.5 for western blotting analysis with antibodies against pMLC. Antibody staining against Myc and GFP shows the levels of dominant-negative ROCK and GFP–MLC, respectively. α-tubulin is loading control. (F) ROCK is required for GEF-H1-mediated SRF-Luc reporter activation. 20 pg of SRF reporter (3DA-SRF-Luc or mutated 2MA-SRF-Luc) DNAs were co-injected with RNAs encoding GEF-H1-C53R (60 pg) and dominant-negative ROCK (250 pg) into two dorsal-animal blastomeres of four-cell embryos, as indicated. The relative luciferase activity was measured in lysates of embryos harvested at stage 10.5. Means±s.d. are shown. Every group included four independent sets, each containing four embryos.

been proposed to induce apical constriction through recruiting ROCK (Mohan et al., 2012; Nishimura and Takeichi, 2008). During chicken lens pit invagination, the ability of Shroom to drive apical constriction has been linked to RhoA and the RhoA GEF Trio (Plageman et al., 2011). Our analysis revealed remarkable similarities between GEF-H1 and Shroom, both in gain- and loss-of-function experiments, suggesting that the two proteins function in the same molecular pathway. Another protein that is involved in both apical constriction and neural tube closure is Lulu, also known as the FERM-domain-containing protein Epb4.1l5 (Chu et al., 2013; Lee et al., 2007b; Nakajima and Tanoue, 2012). In cultured mammalian cells, Lulu can bind to

and stimulate p114GEF (also known as ARHGEF18 in human), leading to ROCK and myosin II activation (Nakajima and Tanoue, 2012). It will be important to confirm the connection between Lulu and p114GEF in diverse experimental models and to test the alternative possibility that Lulu regulates neural tube closure through GEF-H1. Of note, we have previously found that *Xenopus* Lgl1, a polarity protein that binds myosin II, also induces apical constriction and that this activity is under the control of Wnt signaling, but the mechanism of this regulation, and its possible connection to GEF-H1, remains to be clarified (Choi and Sokol, 2009; Dollar et al., 2005). Interestingly, GEF-H1 has been implicated in Wnt3a-dependent neurite retraction
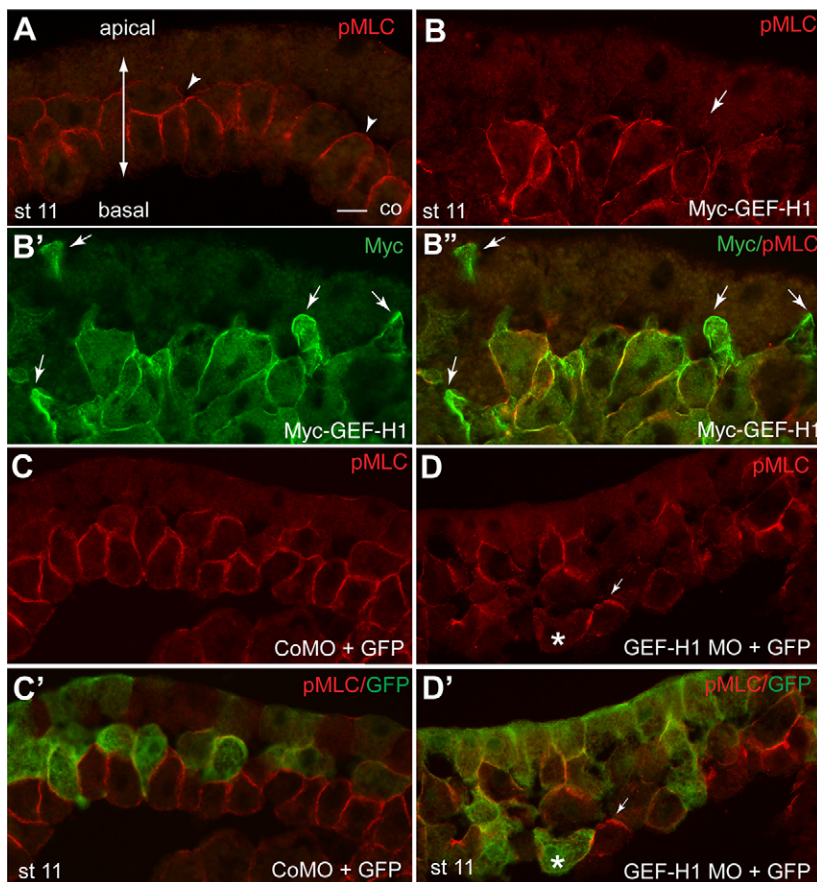
Fig. 8. GEF-H1 regulates protrusive behavior and the polarized distribution of phosphorylated myosin light chain in inner ectoderm cells. (A–D) Immunostaining of transverse ectoderm sections of stage-11 (st 11) embryos that had been injected with the indicated morpholino oligonucleotides (40 ng) or Myc–GEF-H1 mRNA (5–10 pg). GFP is a lineage tracer. (A) In control (Co) ectoderm, phosphorylated MLC (pMLC) is enriched at the apico-lateral boundaries of inner cells (arrowhead). The apical–basal axis is indicated. (B) Overexpression of Myc–GEF-H1 leads to the formation of apical GEF-H1-positive protrusions in inner ectoderm cells (arrow, $n>25$). pMLC staining is shown (red). B′ shows the staining of Myc (green) in the same field as that shown in B. B″ shows the merged image of B and B′. (C,D) The GEF-H1 morpholino oligonucleotide (GEF-H1 MO, D) but not the control morpholino oligonucleotide (CoMO, C) interferes with pMLC (red) polarization and causes disorganized inner cell morphology in the ectoderm of injected embryos ($n>25$). C′ and D′ show merged images of the pMLC staining from the corresponding panel with localization of GFP. * lack of pMLC staining in GEF-H1-depleted cells as compared with that of uninjected cells (arrow). Scale bar: 20 µm.

and found to interact with the components of the Wnt pathway, mammalian DVL1 and DAAM1 (Tsuji et al., 2010).

Besides apical constriction, ectoderm cell intercalation is also altered in GEF-H1 morphants at the gastrula and neurula stages. Multiple cell layers were observed in GEF-H1-depleted embryos, even before the onset of gastrulation, supporting the hypothesis that GEF-H1 is necessary for epiboly, which is largely driven by the radial intercalation of deep cells (Keller, 1980). These early epiboly defects might be later responsible for abnormal neural tube closure in GEF-H1-depleted embryos. Alternatively, these neural tube defects might directly result from inhibited dorsal convergence at late-gastrula and/or early-neurula stages. Surprisingly, we found that ventral injections of GEF-H1 MO also led to incomplete neural tube closure. This suggests that non-neural ectoderm, which fails to converge towards the midline in GEF-H1-depleted embryos, might be partly responsible for the neural plate defects (data not shown). Attesting to the specificity of GEF-H1 in regulating ectodermal cell behaviors, mesodermal convergent extension of activin-induced animal pole explants was not inhibited by GEF-H1 MO. One potential explanation of this result is that GEF-H1 is required specifically for neural convergent extension, whereas WGEF, an unrelated Rho GEF, functions to regulate mesodermal convergent extension (Tanegashima et al., 2008). Although mediolateral cell intercalations are thought to drive dorsal convergence both in mesoderm and neuroectoderm, the mechanisms that regulate this process in different germ layers are poorly understood (Elul et al., 1997; Keller et al., 1992a; Keller et al., 1992b; Keller, 1980).

Our results establish roles for GEF-H1 in multiple signaling processes that regulate cell shape and cell movements during neural tube closure. Surprisingly, mice lacking the *GEF-H1/Lfc* gene do not exhibit neural tube abnormalities (Meiri et al., 2012), suggesting that this protein functions redundantly with other GEFs in neural tube closure. The pleiotropic roles of GEF-H1 in cell intercalations and apical constriction parallel the known functions of myosin II, reiterating the view that myosin II is a major cellular target of GEF-H1. Indeed, the changes in phosphorylated MLC that we observed upon modulation of GEF-H1 indicate that GEF-H1 exerts its effect on both cell intercalation and apical constriction by regulating myosin II activity. Nevertheless, the involvement of GEF-H1 in diverse cell behaviors might, in principle, be due to alternative molecular targets (Birkenfeld et al., 2008). Besides its direct regulation of RhoA, GEF-H1 binds to Cingulin to regulate tight junctions (Aijaz et al., 2005; Benais-Pont et al., 2003; Guillemot et al., 2008). Moreover, GEF-H1 has been identified as a molecular substrate for PAR-1, a component of the apical-basal polarity network (Yamahashi et al., 2011; Yoshimura and Miki, 2011). Based on the interaction of GEF-H1 with the exocyst component Sec5, Pathak and colleagues (Pathak et al., 2012) proposed that the local activation of RhoA by GEF-H1 stimulates exocytosis. Consistent with these findings, we observed that the apical accumulation of Rab11 in the neural plate is lost in GEF-H1-depleted cells. Whereas Rab11 is a strong marker of apical constriction (Ossipova et al., 2014), the causal relationship between GEF-H1-mediated Rab11 recruitment and RhoA

activation is, presently, unclear. Future studies are needed to determine which of the identified molecular targets are involved in the regulation of specific morphogenetic cell behaviors by GEF-H1.

MATERIALS AND METHODS
DNA constructs and morpholinos

The clone for *Xenopus laevis* GEF-H1 was obtained from Open Biosystems (GenBank accession number BC072246). Plasmids encoding the human GEF-H1-C53R and human GEF-H1-Y393A, which were fused to enhanced GFP (Krendel et al., 2002) were a gift from Celine Dermardirossian (Scripps Research Institute, La Jolla, CA). These constructs were subcloned into pXT7 for RNA injections. Pfu-I-directed mutagenesis, followed by *Dpn*I digestion, was performed to generate wild-type human GEF-H1 and *Xenopus* Myc–GEF-H1-Y444A as described previously (Makarova et al., 2000). *Xenopus* GEF-H1a-HA, with and without morpholino oligonucleotide target sequences, were constructed by using 5′-GGTGAATCGGGGATCGTACCCATACG-ATGTTCCAGATTACGCTTCGGAGAGTTAAAGATGC-3′ and 5′-CG-CGTCCGGGCGTATACTCAATGGTCGGTGGGAAATCC-3′ primers, respectively. Myc-GEF-H1 was constructed by subcloning the full-length *Xenopus* GEF-H1a insert into pCS2-Myc. To generate GFP-MLC-pXT7, an insert corresponding to chicken MLC fused with GFP (Ward et al., 2002) was subcloned into the vector pXT7. The other plasmids constructs were pCS2-LacZ, the plasmid pCS2 encoding nuclear *LacZ* (Turner and Weintraub, 1994); pCS2-memRFP, encoding membrane associated RFP (a gift from Sean Megason, Harvard Medical School, Boston, MA); pCS2-mGFP, encoding membrane associated GFP (Ossipova et al., 2007); wild-type and dominant-negative ROCK (Marlow et al., 2002); and pCS2-ShroomL, encoding the long form of Shroom3 (Hildebrand and Soriano, 1999). Details of cloning are available on request.

NCBI database searches identified two *Xenopus laevis* GEF-H1 cDNAs (accession numbers: BC072246 and NM_001136164, which are referred to as GEF-H1a and GEF-H1b, respectively, in this study). The two forms of GEF-H1 diverge only in the 5′-untranslated sequence and several N-terminal amino acids, probably due to alternative splicing. RT-PCR analysis revealed expression of GEF-H1a RNA in gastrula ectoderm as previously reported (Morgan et al., 1999), but GEF-H1b RNA was poorly detectable under the same conditions (data not shown). Therefore, subsequent analysis was restricted to GEF-H1a. For knockdown studies, three different morpholino oligonucleotides were obtained from GeneTools (Ekker, 2000; Heasman et al., 2000) with the following sequences: GEF-H1a MO, 5′-AGGTGCGGTCAATGCCGGACATTGA-3′; GEF-H1 MO, 5′-ACATTGAGACGGATTTGGACAGAGG-3′; GEF-H1b MO, 5′-GGACCACCCTGTTGCTGCATCTTCT-3′. These differ from GEF-H1/Lfc morpholino oligonucleotide sequences that have been reported previously (Kwan and Kirschner, 2005; Zhou et al., 2010). The sequence of the control MO was 5′-GCTTCAGCTAGTGACACATGCAT-3′.

Embryo culture, microinjections, clonal analysis, *in situ* hybridization and animal cap assay

Eggs and embryos were obtained from *Xenopus laevis* and cultured in 0.1×Marc's modified Ringer's solution (MMR) (Newport and Kirschner, 1982) as described previously (Itoh et al., 2005). Staging was performed as described previously (Nieuwkoop and Faber, 1967). For microinjection, embryos were transferred to 3% Ficoll in 0.5×MMR and injected at the 4–8-cell stage with 5–10 nl of a solution containing RNAs and/or morpholino oligonucleotides. Capped synthetic RNAs were generated by *in vitro* transcription with SP6 or T7 RNA polymerase using the mMessage mMachine kit (Ambion) from the corresponding DNA templates.

For clonal analysis, morpholino oligonucleotides against GEF-H1 were injected into one dorsal blastomere of four-cell embryos, followed by injections of *LacZ* RNA into two dorso-lateral blastomeres of 16-cell embryos. β-galactosidase staining was carried out with Red-Gal (Research Organics) and reinforced by bleaching in 1% H$_2$O$_2$, 5% formamide in 0.5× saline sodium citrate buffer, following standard protocols (Harland, 1991). Clone spreading was quantified at stage 11 by comparing the average diameters of β-galactosidase-positive areas on the left (control) and on the right (injected with morpholino oligonucleotide) sides, relative to the whole embryo length.

Ectopic apical constriction was examined at blastula stages after GEF-H1 RNA injections into two animal ventral blastomeres of 4–8 cell embryos. Each group contained 15 to 30 embryos in several independent experiments. Optimal doses of RNAs were determined in separate dose-response experiments for individual RNAs. Whole-mount *in situ* hybridization with an antisense *Sox2* probe (Mizuseki et al., 1998) was performed when the injected embryos reached stages 14–15, as described previously (Harland, 1991). Neural tube defects were quantified by comparing the width of the *Sox2* expression domain at the mid-hindbrain level for the injected and the uninjected sides. Images were taken by using a Leica stereomicroscope and using the Openlab software.

For animal cap assays, injections were carried out into four animal-pole blastomeres at the 4–8-cell stage. When control embryos reached stage 8, ectodermal explants were excised and cultured in 0.1×MMR containing 0.1 mg/ml bovine serum albumin with or without 0.5 ng/ml activin A. The explants were cultured until stages 15–16 to observe elongation phenotypes. Each group consisted of 10–15 explants. These experiments were repeated three times.

Immunostaining and cell shape analysis

For cryosectioning, embryos were devitellinized at the necessary stage, fixed in MEMFA or Dent's fixative for 1–2 hours, and embedded in 15% fish gelatin and 15% sucrose solution as described previously (Ossipova et al., 2007). The embedded embryos were frozen in dry ice and sectioned at 10–12 μm using a Leica CM3050 cryostat. The cell shape in neuroectoderm was analyzed in cryosections that had been stained with an antibody against β-catenin, which marks cell boundary of all cells at neurula stages. The shape of neural plate cells was scored as the ratio of the apical-basal length to the apical width for 5 to 7 superficial cells that were adjacent to the dorsal midline.

For indirect immunofluorescence, embryo sections were stained with a rabbit antibody against β-catenin (Santa Cruz, 1:400), a rabbit antibody against phosphorylated histone 3 (Cell Signaling, 1:200), a mouse antibody against Myc (clone 9E10) (Roche, 1:50 from hybridoma supernatant), a mouse antibody against GFP (clone B2, Santa-Cruz, 1:200), a rabbit antibody against γ-tubulin (Abcam, 1:100), a rabbit antibody against Rab11 (Invitrogen, 1:100), a rabbit antibody against HA (Bethyl Laboratories, 1:2000) and Alexa-Fluor-488-, Alexa-Fluor-555-conjugated (Invitrogen, 1:200) or Cy3-conjugated (Jackson Immunoresearch, 1:200) secondary antibodies. F-actin was detected by using Alexa-Fluor-568-conjugated phalloidin (4 units/ml, Invitrogen). RFP fluorescence was visualized directly without immunostaining. Sections were stained with 1 mg/ml DAPI and mounted by using Vectashield mounting media (Vector). For phosphorylated MLC staining, by using a rabbit antibody against phosphorylated MLC (Abcam, 1:100), gastrula-stage embryos were fixed in 2% trichloroacetic acid (TCA) for 30 min and washed in PBS+0.3% Triton X-100 for 30 min (Nandadasa et al., 2009). For Myc- or HA-tagged GEF-H1 localization, embryos were fixed, cryosectioned and subjected to indirect immunofluorescence. Similar protein localization patterns were observed for differently tagged GEF-H1 constructs using either Dent's or TCA fixatives (data not shown). Staining patterns were reproduced in at least three independent experiments. Representative sections of experimental groups (each containing 10–15 embryos) are shown. Imaging was performed by using a Zeiss AxioImager microscope.

Western blotting analysis and luciferase assays

Western blotting analysis was performed using standard techniques as described previously (Itoh et al., 2000). Four-cell to eight-cell embryos were injected with RNAs encoding GFP–GEF-H1-C53R, GFP–GEF-H1-Y393A, GFP–MLC, wild-type or Myc–dominant-negative-ROCK. Whole lysates were prepared from five embryos at stage 8.5 or 10.5–11. For testing morpholino oligonucleotide specificity, four animal-pole blastomeres of 4–8-cell embryos were injected with *Xenopus* GEF-H1-HA RNA±GEF-H1a MO, GEF-H1 MO or control MO, and whole

lysates were prepared from six embryos at stage 10+. The antibodies used were against phosphorylated MLC (Abcam, 1 in 500), Myc (clone 9E10, Roche, 1 in 200), HA (clone 12CA5, Roche, 1 in 200), GFP (Santa Cruz, clone B2, 1/1000) and α-tubulin (Sigma, 1 in 100,000).

For luciferase activity assays, 20 pg of plasmid DNA for the SRF reporter p3DA.luc or the mutated control reporter p2MA.luc (Busche et al., 2008; Posern et al., 2002) was co-injected with GEF-H1-C53R and/or dominant-negative ROCK RNAs into two dorsal-animal blastomeres at the 4–8-cell stage. Luciferase activity was measured when sibling embryos reached stage 11, as described previously (Fan et al., 1998).

Author contributions
K.I., O.O. and S.S. designed the experiments, analyzed the data and wrote the manuscript. K. I. and O. O. performed the experiments.

Supplementary material
Supplementary material available online at
http://jcs.biologists.org/lookup/suppl/doi:10.1242/jcs.146811/-/DC1

References
Aijaz, S., D'Atri, F., Citi, S., Balda, M. S. and Matter, K. (2005). Binding of GEF-H1 to the tight junction-associated adaptor cingulin results in inhibition of Rho signaling and G1/S phase transition. Dev. Cell 8, 777-786.
Barrett, K., Leptin, M. and Settleman, J. (1997). The Rho GTPase and a putative RhoGEF mediate a signaling pathway for the cell shape changes in Drosophila gastrulation. Cell 91, 905-915.
Benais-Pont, G., Punn, A., Flores-Maldonado, C., Eckert, J., Raposo, G., Fleming, T. P., Cereijido, M., Balda, M. S. and Matter, K. (2003). Identification of a tight junction-associated guanine nucleotide exchange factor that activates Rho and regulates paracellular permeability. J. Cell Biol. 160, 729-740.
Birkenfeld, J., Nalbant, P., Bohl, B. P., Pertz, O., Hahn, K. M. and Bokoch, G. M. (2007). GEF-H1 modulates localized RhoA activation during cytokinesis under the control of mitotic kinases. Dev. Cell 12, 699-712.
Birkenfeld, J., Nalbant, P., Yoon, S. H. and Bokoch, G. M. (2008). Cellular functions of GEF-H1, a microtubule-regulated Rho-GEF: is altered GEF-H1 activity a crucial determinant of disease pathogenesis? Trends Cell Biol. 18, 210-219.
Birukova, A. A., Adyshev, D., Gorshkov, B., Bokoch, G. M., Birukov, K. G. and Verin, A. D. (2006). GEF-H1 is involved in agonist-induced human pulmonary endothelial barrier dysfunction. Am. J. Physiol. 290, L540-L548.
Busche, S., Descot, A., Julien, S., Genth, H. and Posern, G. (2008). Epithelial cell-cell contacts regulate SRF-mediated transcription via Rac-actin-MAL signalling. J. Cell Sci. 121, 1025-1035.
Chang, Y. C., Nalbant, P., Birkenfeld, J., Chang, Z. F. and Bokoch, G. M. (2008). GEF-H1 couples nocodazole-induced microtubule disassembly to cell contractility via RhoA. Mol. Biol. Cell 19, 2147-2153.
Choi, S. C. and Sokol, S. Y. (2009). The involvement of lethal giant larvae and Wnt signaling in bottle cell formation in Xenopus embryos. Dev. Biol. 336, 68-75.
Chu, C. W., Gerstenzang, E., Ossipova, O. and Sokol, S. Y. (2013). Lulu regulates Shroom-induced apical constriction during neural tube closure. PLoS ONE 8, e81854.
Colas, J. F. and Schoenwolf, G. C. (2001). Towards a cellular and molecular understanding of neurulation. Dev. Dyn. 221, 117-145.
Davidson, L. A. and Keller, R. E. (1999). Neural tube closure in Xenopus laevis involves medial migration, directed protrusive activity, cell intercalation and convergent extension. Development 126, 4547-4556.
De Robertis, E. M. and Kuroda, H. (2004). Dorsal-ventral patterning and neural induction in Xenopus embryos. Annu. Rev. Cell Dev. Biol. 20, 285-308.
Dollar, G. L., Weber, U., Mlodzik, M. and Sokol, S. Y. (2005). Regulation of lethal giant larvae by dishevelled. Nature 437, 1376-1380.
Ekker, S. C. (2000). Morphants: a new systematic vertebrate functional genomics approach. Yeast 17, 302-306.
Elul, T., Koehl, M. A. and Keller, R. (1997). Cellular mechanism underlying neural convergent extension in Xenopus laevis embryos. Dev. Biol. 191, 243-258.

Fan, M. J., Grüning, W., Walz, G. and Sokol, S. Y. (1998). Wnt signaling and transcriptional control of Siamois in Xenopus embryos. Proc. Natl. Acad. Sci. USA 95, 5626-5631.
Glaven, J. A., Whitehead, I., Bagrodia, S., Kay, R. and Cerione, R. A. (1999). The Dbl-related protein, Lfc, localizes to microtubules and mediates the activation of Rac signaling pathways in cells. J. Biol. Chem. 274, 2279-2285.
Gray, R. S., Roszko, I. and Solnica-Krezel, L. (2011). Planar cell polarity: coordinating morphogenetic cell behaviors with embryonic polarity. Dev. Cell 21, 120-133.
Guillemot, L., Paschoud, S., Jond, L., Foglia, A. and Citi, S. (2008). Paracingulin regulates the activity of Rac1 and RhoA GTPases by recruiting Tiam1 and GEF-H1 to epithelial junctions. Mol. Biol. Cell 19, 4442-4453.
Habas, R., Kato, Y. and He, X. (2001). Wnt/Frizzled activation of Rho regulates vertebrate gastrulation and requires a novel Formin homology protein Daam1. Cell 107, 843-854.
Habas, R., Dawid, I. B. and He, X. (2003). Coactivation of Rac and Rho by Wnt/Frizzled signaling is required for vertebrate gastrulation. Genes Dev. 17, 295-309.
Häcker, U. and Perrimon, N. (1998). DRhoGEF2 encodes a member of the Dbl family of oncogenes and controls cell shape changes during gastrulation in Drosophila. Genes Dev. 12, 274-284.
Haigo, S. L., Hildebrand, J. D., Harland, R. M. and Wallingford, J. B. (2003). Shroom induces apical constriction and is required for hingepoint formation during neural tube closure. Curr. Biol. 13, 2125-2137.
Hall, A. (2005). Rho GTPases and the control of cell behaviour. Biochem. Soc. Trans. 33, 891-895.
Harland, R. M. (1991). In situ hybridization: an improved whole-mount method for Xenopus embryos. Methods Cell Biol. 36, 685-695.
Harris, M. J. and Juriloff, D. M. (2010). An update to the list of mouse mutants with neural tube closure defects and advances toward a complete genetic perspective of neural tube closure. Birth Defects Res. A Clin. Mol. Teratol. 88, 653-669.
Heasman, J., Kofron, M. and Wylie, C. (2000). Beta-catenin signaling activity dissected in the early Xenopus embryo: a novel antisense approach. Dev. Biol. 222, 124-134.
Heasman, S. J., Carlin, L. M., Cox, S., Ng, T. and Ridley, A. J. (2010). Coordinated RhoA signaling at the leading edge and uropod is required for T cell transendothelial migration. J. Cell Biol. 190, 553-563.
Hildebrand, J. D. (2005). Shroom regulates epithelial cell shape via the apical positioning of an actomyosin network. J. Cell Sci. 118, 5191-5203.
Hildebrand, J. D. and Soriano, P. (1999). Shroom, a PDZ domain-containing actin-binding protein, is required for neural tube morphogenesis in mice. Cell 99, 485-497.
Howard, J. E. and Smith, J. C. (1993). Analysis of gastrulation: different types of gastrulation movement are induced by different mesoderm-inducing factors in Xenopus laevis. Mech. Dev. 43, 37-48.
Itoh, K., Antipova, A., Ratcliffe, M. J. and Sokol, S. (2000). Interaction of dishevelled and Xenopus axin-related protein is required for wnt signal transduction. Mol. Cell. Biol. 20, 2228-2238.
Itoh, K., Brott, B. K., Bae, G. U., Ratcliffe, M. J. and Sokol, S. Y. (2005). Nuclear localization is required for Dishevelled function in Wnt/beta-catenin signaling. J. Biol. 4, 3.
Jaffe, A. B. and Hall, A. (2005). Rho GTPases: biochemistry and biology. Annu. Rev. Cell Dev. Biol. 21, 247-269.
Kashef, J., Köhler, A., Kuriyama, S., Alfandari, D., Mayor, R. and Wedlich, D. (2009). Cadherin-11 regulates protrusive activity in Xenopus cranial neural crest cells upstream of Trio and the small GTPases. Genes Dev. 23, 1393-1398.
Keller, R. E. (1980). The cellular basis of epiboly: an SEM study of deep-cell rearrangement during gastrulation in Xenopus laevis. J. Embryol. Exp. Morphol. 60, 201-234.
Keller, R. (1991). Early embryonic development of Xenopus laevis. Methods Cell Biol. 36, 61-113.
Keller, R. (2002). Shaping the vertebrate body plan by polarized embryonic cell movements. Science 298, 1950-1954.
Keller, R., Shih, J. and Sater, A. (1992a). The cellular basis of the convergence and extension of the Xenopus neural plate. Dev. Dyn. 193, 199-217.
Keller, R., Shih, J., Sater, A. K. and Moreno, C. (1992b). Planar induction of convergence and extension of the neural plate by the organizer of Xenopus. Dev. Dyn. 193, 218-234.
Kinoshita, N., Sasai, N., Misaki, K. and Yonemura, S. (2008). Apical accumulation of Rho in the neural plate is important for neural plate cell shape change and neural tube formation. Mol. Biol. Cell 19, 2289-2299.
Kölsch, V., Seher, T., Fernandez-Ballester, G. J., Serrano, L. and Leptin, M. (2007). Control of Drosophila gastrulation by apical localization of adherens junctions and RhoGEF2. Science 315, 384-386.
Krendel, M., Zenke, F. T. and Bokoch, G. M. (2002). Nucleotide exchange factor GEF-H1 mediates cross-talk between microtubules and the actin cytoskeleton. Nat. Cell Biol. 4, 294-301.
Kwan, K. M. and Kirschner, M. W. (2005). A microtubule-binding Rho-GEF controls cell morphology during convergent extension of Xenopus laevis. Development 132, 4599-4610.
Lecuit, T., Lenne, P. F. and Munro, E. (2011). Force generation, transmission, and integration during cell and tissue morphogenesis. Annu. Rev. Cell Dev. Biol. 27, 157-184.
Lee, J. Y. and Harland, R. M. (2007). Actomyosin contractility and microtubules drive apical constriction in Xenopus bottle cells. Dev. Biol. 311, 40-52.

Lee, C., Scherr, H. M. and Wallingford, J. B. (2007a). Shroom family proteins regulate gamma-tubulin distribution and microtubule architecture during epithelial cell shape change. *Development* **134**, 1431-1441.

Lee, J. D., Silva-Gagliardi, N. F., Tepass, U., McGlade, C. J. and Anderson, K. V. (2007b). The FERM protein Epb4.1l5 is required for organization of the neural plate and for the epithelial-mesenchymal transition at the primitive streak of the mouse embryo. *Development* **134**, 2007-2016.

Makarova, O., Kamberov, E. and Margolis, B. (2000). Generation of deletion and point mutations with one primer in a single cloning step. *Biotechniques* **29**, 970-972.

Marlow, F., Topczewski, J., Sepich, D. and Solnica-Krezel, L. (2002). Zebrafish Rho kinase 2 acts downstream of Wnt11 to mediate cell polarity and effective convergence and extension movements. *Curr. Biol.* **12**, 876-884.

Meiri, D., Marshall, C. B., Greeve, M. A., Kim, B., Balan, M., Suarez, F., Bakal, C., Wu, C., Larose, J., Fine, N. et al. (2012). Mechanistic insight into the microtubule and actin cytoskeleton coupling through dynein-dependent RhoGEF inhibition. *Mol. Cell* **45**, 642-655.

Miyakoshi, A., Ueno, N. and Kinoshita, N. (2004). Rho guanine nucleotide exchange factor xNET1 implicated in gastrulation movements during Xenopus development. *Differentiation* **72**, 48-55.

Mizuseki, K., Kishi, M., Matsui, M., Nakanishi, S. and Sasai, Y. (1998). Xenopus Zic-related-1 and Sox-2, two factors induced by chordin, have distinct activities in the initiation of neural induction. *Development* **125**, 579-587.

Mohan, S., Rizaldy, R., Das, D., Bauer, R. J., Heroux, A., Trakselis, M. A., Hildebrand, J. D. and VanDemark, A. P. (2012). Structure of Shroom domain 2 reveals a three-segmented coiled-coil required for dimerization, Rock binding, and apical constriction. *Mol. Biol. Cell* **23**, 2131-2142.

Morgan, R., Hooiveld, M. H. and Durston, A. J. (1999). A novel guanine exchange factor increases the competence of early ectoderm to respond to neural induction. *Mech. Dev.* **88**, 67-72.

Nakajima, H. and Tanoue, T. (2012). The circumferential actomyosin belt in epithelial cells is regulated by the Lulu2-p114RhoGEF system. *Small GTPases* **3**, 91-96.

Nalbant, P., Chang, Y. C., Birkenfeld, J., Chang, Z. F. and Bokoch, G. M. (2009). Guanine nucleotide exchange factor-H1 regulates cell migration via localized activation of RhoA at the leading edge. *Mol. Biol. Cell* **20**, 4070-4082.

Nandadasa, S., Tao, Q., Menon, N. R., Heasman, J. and Wylie, C. (2009). N- and E-cadherins in Xenopus are specifically required in the neural and non-neural ectoderm, respectively, for F-actin assembly and morphogenetic movements. *Development* **136**, 1327-1338.

Newport, J. and Kirschner, M. (1982). A major developmental transition in early Xenopus embryos: I. characterization and timing of cellular changes at the midblastula stage. *Cell* **30**, 675-686.

Nieuwkoop, P. D. and Faber, J. (1967). *Normal Table of Xenopus Laevis (Daudin)*. Amsterdam: North Holland.

Nishimura, T. and Takeichi, M. (2008). Shroom3-mediated recruitment of Rho kinases to the apical cell junctions regulates epithelial and neuroepithelial planar remodeling. *Development* **135**, 1493-1502.

Nishimura, T., Honda, H. and Takeichi, M. (2012). Planar cell polarity links axes of spatial dynamics in neural-tube closure. *Cell* **149**, 1084-1097.

Ossipova, O., Tabler, J., Green, J. B. and Sokol, S. Y. (2007). PAR1 specifies ciliated cells in vertebrate ectoderm downstream of aPKC. *Development* **134**, 4297-4306.

Ossipova, O., Kim, K., Lake, B. B., Itoh, K., Ioannou, A. and Sokol, S. Y. (2014). Role of Rab11 in planar cell polarity and apical constriction during vertebrate neural tube closure. *Nat. Commun.* 5:3734, doi: 10.1038/ncomms4734.

Panizzi, J. R., Jessen, J. R., Drummond, I. A. and Solnica-Krezel, L. (2007). New functions for a vertebrate Rho guanine nucleotide exchange factor in ciliated epithelia. *Development* **134**, 921-931.

Pathak, R., Delorme-Walker, V. D., Howell, M. C., Anselmo, A. N., White, M. A., Bokoch, G. M. and Dermardirossian, C. (2012). The microtubule-associated Rho activating factor GEF-H1 interacts with exocyst complex to regulate vesicle traffic. *Dev. Cell* **23**, 397-411.

Plageman, T. F., Jr, Chauhan, B. K., Yang, C., Jaudon, F., Shang, X., Zheng, Y., Lou, M., Debant, A., Hildebrand, J. D. and Lang, R. A. (2011). A Trio-RhoA-Shroom3 pathway is required for apical constriction and epithelial invagination. *Development* **138**, 5177-5188.

Posern, G. and Treisman, R. (2006). Actin' together: serum response factor, its cofactors and the link to signal transduction. *Trends Cell Biol.* **16**, 588-596.

Posern, G., Sotiropoulos, A. and Treisman, R. (2002). Mutant actins demonstrate a role for unpolymerized actin in control of transcription by serum response factor. *Mol. Biol. Cell* **13**, 4167-4178.

Poznanski, A., Minsuk, S., Stathopoulos, D. and Keller, R. (1997). Epithelial cell wedging and neural trough formation are induced planarly in Xenopus, without persistent vertical interactions with mesoderm. *Dev. Biol.* **189**, 256-269.

Rauzi, M., Lenne, P. F. and Lecuit, T. (2010). Planar polarized actomyosin contractile flows control epithelial junction remodelling. *Nature* **468**, 1110-1114.

Ren, Y., Li, R., Zheng, Y. and Busch, H. (1998). Cloning and characterization of GEF-H1, a microtubule-associated guanine nucleotide exchange factor for Rac and Rho GTPases. *J. Biol. Chem.* **273**, 34954-34960.

Rolo, A., Skoglund, P. and Keller, R. (2009). Morphogenetic movements driving neural tube closure in Xenopus require myosin IIB. *Dev. Biol.* **327**, 327-338.

Rossman, K. L., Der, C. J. and Sondek, J. (2005). GEF means go: turning on RHO GTPases with guanine nucleotide-exchange factors. *Nat. Rev. Mol. Cell Biol.* **6**, 167-180.

Saka, Y. and Smith, J. C. (2001). Spatial and temporal patterns of cell division during early Xenopus embryogenesis. *Dev. Biol.* **229**, 307-318.

Sawyer, J. M., Harrell, J. R., Shemer, G., Sullivan-Brown, J., Roh-Johnson, M. and Goldstein, B. (2010). Apical constriction: a cell shape change that can drive morphogenesis. *Dev. Biol.* **341**, 5-19.

Schroeder, T. E. (1970). Neurulation in Xenopus laevis. An analysis and model based upon light and electron microscopy. *J. Embryol. Exp. Morphol.* **23**, 427-462.

Sokol, S. Y. (1996). Analysis of Dishevelled signalling pathways during Xenopus development. *Curr. Biol.* **6**, 1456-1467.

Suzuki, M., Morita, H. and Ueno, N. (2012). Molecular mechanisms of cell shape changes that contribute to vertebrate neural tube closure. *Dev. Growth Differ.* **54**, 266-276.

Tanegashima, K., Zhao, H. and Dawid, I. B. (2008). WGEF activates Rho in the Wnt-PCP pathway and controls convergent extension in Xenopus gastrulation. *EMBO J.* **27**, 606-617.

Tsapara, A., Luthert, P., Greenwood, J., Hill, C. S., Matter, K. and Balda, M. S. (2010). The RhoA activator GEF-H1/Lfc is a transforming growth factor-beta target gene and effector that regulates alpha-smooth muscle actin expression and cell migration. *Mol. Biol. Cell* **21**, 860-870.

Tsuji, T., Ohta, Y., Kanno, Y., Hirose, K., Ohashi, K. and Mizuno, K. (2010). Involvement of p114-RhoGEF and Lfc in Wnt-3a- and dishevelled-induced RhoA activation and neurite retraction in N1E-115 mouse neuroblastoma cells. *Mol. Biol. Cell* **21**, 3590-3600.

Tullio, A. N., Bridgman, P. C., Tresser, N. J., Chan, C. C., Conti, M. A., Adelstein, R. S. and Hara, Y. (2001). Structural abnormalities develop in the brain after ablation of the gene encoding nonmuscle myosin II-B heavy chain. *J. Comp. Neurol.* **433**, 62-74.

Turner, D. L. and Weintraub, H. (1994). Expression of achaete-scute homolog 3 in Xenopus embryos converts ectodermal cells to a neural fate. *Genes Dev.* **8**, 1434-1447.

Vicente-Manzanares, M., Ma, X., Adelstein, R. S. and Horwitz, A. R. (2009). Non-muscle myosin II takes centre stage in cell adhesion and migration. *Nat. Rev. Mol. Cell Biol.* **10**, 778-790.

Wallingford, J. B., Niswander, L. A., Shaw, G. M. and Finnell, R. H. (2013). The continuing challenge of understanding, preventing, and treating neural tube defects. *Science* **339**, 1222002.

Ward, Y., Yap, S. F., Ravichandran, V., Matsumura, F., Ito, M., Spinelli, B. and Kelly, K. (2002). The GTP binding proteins Gem and Rad are negative regulators of the Rho-Rho kinase pathway. *J. Cell Biol.* **157**, 291-302.

Yamahashi, Y., Saito, Y., Murata-Kamiya, N. and Hatakeyama, M. (2011). Polarity-regulating kinase partitioning-defective 1b (PAR1b) phosphorylates guanine nucleotide exchange factor H1 (GEF-H1) to regulate RhoA-dependent actin cytoskeletal reorganization. *J. Biol. Chem.* **286**, 44576-44584.

Yoshimura, Y. and Miki, H. (2011). Dynamic regulation of GEF-H1 localization at microtubules by Par1b/MARK2. *Biochem. Biophys. Res. Commun.* **408**, 322-328.

Zhou, J., Kim, H. Y., Wang, J. H. and Davidson, L. A. (2010). Macroscopic stiffening of embryonic tissues via microtubules, RhoGEF and the assembly of contractile bundles of actomyosin. *Development* **137**, 2785-2794.